Heat source layout optimization for two-dimensional heat conduction using iterative reweighted L1-norm convex minimization

Aslan, Yanki; Puskely, Jan; Yarovoy, Alexander

DOI
10.1016/j.ijheatmasstransfer.2018.02.001

Publication date
2018

Document Version
Final published version

Published in
International Journal of Heat and Mass Transfer

International Journal of Heat and Mass Transfer 122 (2018) 432–441

Contents lists available at ScienceDirect

International Journal of Heat and Mass Transfer

journal homepage: www.elsevier.com/locate/ijhmt

Heat source layout optimization for two-dimensional heat conduction using iterative reweighted L1-norm convex minimization

Yanki Aslan *, Jan Puskely, Alexander Yarovoy

Microwave Sensing, Signals and Systems Group, Department of Microelectronics, Faculty of Electrical Engineering, Mathematics and Computer Science, Delft University of Technology, Mekelweg 4, 2628 CD Delft, The Netherlands

ARTICLE INFO

Article history:
Received 12 September 2017
Received in revised form 29 January 2018
Accepted 1 February 2018
Available online 7 February 2018

Keywords:
Heat source layout
Heat conduction optimization
Compressed sensing
Sequential convex optimization

ABSTRACT

Optimization of heat source distribution in two dimensional heat conduction for electronic cooling problem is considered. Convex optimization is applied to this problem for the first time by reformulating the objective function and the non-convex constraints. Mathematical analysis is performed to describe the heat source equation and the combinatorial optimization problem. A sparsity based convex optimization technique is used to solve the problem approximately. The performance of the algorithm is tested by several cases with various boundary conditions and the results are compared with a uniformly distributed layout. These results indicate that through proper selection of the number of grid cells for placing the heat sources and a minimum inter-source spacing, the maximum temperature and temperature non-uniformity in the domain can be significantly reduced. To further assess the capabilities of the method, comparisons to the results available in the literature are also performed. Compared to the existing heat source layout optimization methods, the proposed algorithm can be implemented more easily using available convex programming tools and reduces the number of input control parameters and thus computation time and resources while achieving a similar or better cooling performance.

1. Introduction

During operation of all electronic devices and circuits, certain amount of excess heat is generated. The maximum temperature of the electronics and the temperature uniformity of the domain are important criteria that affect the operation consistency and life of the devices. In order to improve reliability of device operation, unify electronic circuit aging processes and reduce electronics failure probability, thermal management of the overall system is required to be studied. Thermal management deals with dissipating the generated heat efficiently and reducing the maximum temperature of the electronics while approaching a uniform temperature distribution in the domain. The need for thermal management is even more crucial with the fast development of today's electronic production and component integration technology in which the size of the electronics has become smaller and the power density has increased noticeably.

One effective way to enhance the heat conduction performance of the system and reduce the maximum temperature of the domain is to insert highly thermal conductive materials such as diamond or carbon fiber [1,2] that are able to reduce the local thermal resistance. In this case, the distribution of such materials is to be optimized with the aim of minimizing the maximum temperature. A variety of approaches have been discussed in the literature including the constructal theory [3–5], entransy theory [6–8], bionic optimization [9,10] and combinatorial algorithms [11,12]. The results of these algorithms have shown that the optimized conduction path formed by the inserted materials has a shape similar to a tree with several branches varying in number and size.

Although conduction cooling employing high thermal conductivity materials has been shown to be an effective method, the optimal distribution of such materials are difficult to realize in practice and the design costs may increase. An alternative approach is to provide passive cooling via surface heat emission or convection and by optimizing only the positions of the electronics (or the heat sources).

For layout optimization problems with large numbers of degrees of freedom, combinatorial algorithms such as genetic algorithm with artificial neural network [13–16] and particle swarm optimization [17] have been used in the literature. In their recent studies, Chen et al. applied bionic optimization [18,19] and simulated annealing [20] methods to find out the optimal source distribution for varying number (up to several tens) of heat sources, which provided significant reduction in the maximum tempera-

* Corresponding author.
E-mail address: Y.Aslan@tudelft.nl (Y. Aslan).

https://doi.org/10.1016/j.ijheatmasstransfer.2018.02.001
0017-9310/

Nomenclature

Δ	thickness of the domain and the heat sources in the 3D model, m
δ	domain extension length for the heat sink realization in the 3D model, m
ϵ	parameter for the algorithm stability, 1
Γ	area of a single heat source, m^2
ϕ	heat source distribution function, W/m^2
Φ_0	volume heat density of a single heat source in the 3D model, $W/(m^3{\cdot}K)$
ϕ_0	intensity of a single heat source, W/m^2
ϕ_b	background heat source distribution before adding the heat sources, W/m^2
σ	standard deviation of the temperature field in the domain, 1
σ_m	normalized standard deviation of the temperature field in the domain, 1
$\mathbf{w}$	vector $(N_g \times 1)$ of selection weights (within [0,1]) of grid cells, 1
ε	surface emissivity coefficient, 1
d_g	guaranteed minimum inter-source spacing defined at the algorithm input, m
$d_{\min}$	resulting minimum inter-source spacing at the algorithm output, m
h	convective heat transfer coefficient, $W/(m^2{\cdot}K)$
k	thermal conductivity, W/(m·K)
L	side length of the square domain, m
l	side length of a square-shaped heat source, m
N_g	number of grid cells for placing the heat sources, 1
N_s	number of heat sources placed in the domain, 1
N_T	number of temperature field samples in the domain, 1
R_m	normalized maximum temperature rise, 1
S	separation matrix $(N_g \times N_g)$ defining the minimum inter-source spacing, 1
T	temperature field, K
T_0	environmental temperature, K
T_b	background temperature field before adding the heat sources, K
T_i	temperature rise due to adding the ith source, K
t_T	computation time for the resulting temperature field after the optimization, s
T_{avg}	average temperature of the domain, K
$T_{\max}$	maximum temperature of the domain, K
t_{opt}	total computation time for the optimization with the minimum required number of iterations, s
T_{ref}	reference temperature field with uniform heat generation in the domain, K
t_{ref}	computation time for the reference temperature field calculation, s
w_j	selection weight of the source on the jth grid cell, 1
x, y	horizontal and vertical coordinates of the domain, m
$Z^{(j)}$	diagonal weighting matrix $(N_g \times N_g)$ in the jth iteration of the optimization

ture of the domain when compared to the randomly or uniformly distributed heat sources.

In this paper, the layout optimization is addressed using a new method that has not been investigated in the literature. The solution algorithm is based on the sequential reweighted l_1-norm minimization technique. This technique was first introduced by Candes et al. [21] with the aim of minimizing a convex measure of the l_0-norm which is equal to the cardinality of the sources. Recently, the sequential convex optimization method has been effectively used in the domain of sparse antenna array synthesis [22–24] in order to optimize the positions and excitations of the antenna elements. Considering the amplifiers powering the antennas as heat sources, a direct analogy can be made with the heat conduction problem.

Motivated by this analogy, the mathematical modeling of the two-dimensional heat conduction problem is performed and the positions of the heat sources are optimized using the convex optimization algorithm iteratively. The performance is tested using three typical cases with various boundary conditions that were previously applied by Chen et al. [18–20] and an additional case which takes into account the heat emission from the domain surface by convection or radiation while solving the conduction problem.

The remaining parts of the paper are organized as follows. Section 2 presents the mathematical modeling of the two-dimensional heat conduction problem. Section 3 explains the formulation of the layout optimization problem via sequential convex optimizations. Section 4 shows and discusses the results of the four test cases. Section 5 presents the conclusions.

2. Mathematical modeling of the problem

In this section, the mathematical model for the heat conduction optimization problem in a two-dimensional rectangular domain is revised. As previously stated by Chen et al. [18–20], the temperature field (T) satisfies the following equation at steady state

$$\begin{aligned} &\frac{\partial}{\partial x}\left(k\frac{\partial T}{\partial x}\right)+\frac{\partial}{\partial y}\left(k\frac{\partial T}{\partial y}\right)+\phi(x,y)=0 \\ &\text{Boundary}: \quad T=T_0 \quad or \quad k\frac{\partial T}{\partial \mathbf{n}}=0 \quad or \quad k\frac{\partial T}{\partial \mathbf{n}}=h(T-T_0) \end{aligned} \tag{1}$$

where k is the thermal conductivity of the domain, ϕ is the heat source distribution function and T_0 is the temperature value at the isothermal boundary or the fluid temperature at the convective boundary. h represents the convective heat transfer coefficient. In fact, Eq. (1) represents a Poisson problem with Dirichlet (isothermal), Neumann (adiabatic) or Robin (convective) boundary conditions that can be solved with a MATLAB-based finite-difference solver [25].

The heat sources in this study are modeled similar to [18] as follows

$$\phi(x,y)=\begin{cases}\phi_0, & (x,y)\in\Gamma\\ 0, & (x,y)\notin\Gamma\end{cases} \tag{2}$$

where ϕ_0 is the (constant) intensity of a single heat source and Γ represents the area of that heat source.

If a background temperature T_b and a source distribution ϕ_b are assumed, Eq. (1) can be expressed as

$$\begin{aligned} &\frac{\partial}{\partial x}\left(k\frac{\partial T_b}{\partial x}\right)+\frac{\partial}{\partial y}\left(k\frac{\partial T_b}{\partial y}\right)+\phi_b(x,y)=0 \\ &\text{Boundary}: \quad T_b=T_0 \quad or \quad k\frac{\partial T_b}{\partial \mathbf{n}}=0 \quad or \quad k\frac{\partial T_b}{\partial \mathbf{n}}=h(T_b-T_0) \end{aligned} \tag{3}$$

When the ith source is added into the domain, the temperature rise T_i is given by

$$\begin{aligned} &\frac{\partial}{\partial x}\left(k\frac{\partial T_i}{\partial x}\right)+\frac{\partial}{\partial y}\left(k\frac{\partial T_i}{\partial y}\right)+\phi_i(x,y)=0 \\ &\text{Boundary}: \quad T_i=0 \quad or \quad k\frac{\partial T_i}{\partial \mathbf{n}}=0 \quad or \quad k\frac{\partial T_i}{\partial \mathbf{n}}=hT_i \end{aligned} \tag{4}$$

Eq. (4) shows that the temperature rise field (T_i) for the source i is independent of T_b, ϕ_b and T_0. Thus, the combinatorial optimization problem of the heat source distribution can be expressed as follows

$$\begin{aligned} &\text{minimize } (\max(T)) \quad s.t. \\ &T = T_b + \sum_{j=1}^{N_g} w_j T_j \\ &w_j = 0 \quad or \quad 1, \quad j = 1, \ldots, N_g \end{aligned} \tag{5}$$

where w_j is the (binary) selection weight of the source at the jth grid cell, T_j is the respective temperature rise and N_g is the number of grid cells suitable for the heat sources.

Normalization of the variables was also performed by Chen et al. [18] in order to investigate the effect of ϕ_0 and k on the optimized layout. For a square computational domain with side lengths L, the normalized variables are given by

$$\overline{R} = \frac{T - T_0}{\phi_0 L^2/k}, \quad \overline{x} = \frac{x}{L}, \quad \overline{y} = \frac{y}{L}, \quad \overline{\phi} = \frac{\phi}{\phi_0} \tag{6}$$

Using Eq. (6), Eqs. (1) and (2) are represented as

$$\begin{aligned} &\frac{\partial}{\partial \overline{x}}\left(k\frac{\partial \overline{R}}{\partial \overline{x}}\right) + \frac{\partial}{\partial \overline{y}}\left(k\frac{\partial \overline{R}}{\partial \overline{y}}\right) + \overline{\phi}(\overline{x}, \overline{y}) = 0, \\ &\overline{\phi}(\overline{x}, \overline{y}) = \begin{cases} 1, & (\overline{x}, \overline{y}) \in \overline{\Gamma}(\overline{l}) \\ 0, & (\overline{x}, \overline{y}) \notin \overline{\Gamma}(\overline{l}) \end{cases} \\ &\text{Boundary}: \quad \overline{R} = 0 \quad or \quad k\frac{\partial \overline{R}}{\partial \mathbf{n}} = 0 \quad or \quad k\frac{\partial \overline{R}}{\partial \mathbf{n}} = \frac{hL}{k}\overline{R} \end{aligned} \tag{7}$$

The performance is evaluated considering two normalized metrics: normalized maximum temperature rise (R_m) and normalized standard deviation (σ_m) which are defined as

$$R_m = \frac{T_{\max} - T_0}{\phi_0 L^2/k}, \quad \sigma_m = \frac{1}{\phi_0 L^2/k}\sqrt{\frac{1}{N_T}\sum_{i=1}^{N_T}(T_i - T_{\text{avg}})^2} \tag{8}$$

where N_T is the total number of temperature field samples in the domain and T_{avg} is the average temperature value.

3. Problem solution via sequential convex optimizations

The combinatorial problem in Eq. (5) is an NP-hard problem. The main challenge here is the nonconvexity of the objective function resulting from the binary selection weights (i.e. $w_j \in \{0, 1\}$). Motivated by this challenge, an alternative method is proposed in this study which is based on convex relaxation of the binary selection weights (i.e. $w_j \in [0, 1]$) and an approximation of the objective function in Eq. (5) through sequential convex minimization of the weighted l_1-norm of a function given by

$$f = T_{\text{ref}}.\mathbf{w} \tag{9}$$

where T_{ref} is a vector (of length N_g) showing the temperature distribution obtained from a uniform heat generation in the whole domain, or when the domain is densely filled with equal-intensity heat sources. As previously stated, the vector $\mathbf{w}$ contains the relaxed selection weights that could be equal to any value between 0 and 1. The dot product (".") is obtained via element-wise multiplication of the two vectors, which is simply multiplying the temperature value at any grid point by its selection weight.

The logic behind the selection of such an objective function can be demonstrated through solving Eq. (4), which basically shows that the maximum temperature rise takes place at the area of the added heat source. Therefore, T_{ref} in Eq. (9) shows which regions inside the domain are 'easy-to-cool' and which are potentially inefficient in terms of heat conduction. The idea is to select the sources in 'easy-to-cool' regions with larger weights while assigning smaller weights for the areas with high reference temperature.

Having selected the objective function, the challenge now is to decide on the constraints. Note that in the convex optimization algorithm, the domain is discretized with N_g cells and there is a heat source placed at each cell on the grid. The difference is in the selection weights of the sources. For the ideal case in which the number of sources (N_s) is identified, N_s sources are selected with weight 1 and the remaining ($N_g - N_s$) sources are selected with weight 0. Therefore, the convex algorithm should yield a sparse solution in terms of the selection weights ($\mathbf{w}$) to remove $N_g - N_s$ heat sources. Besides, the heat sources should not overlap in the final layout, which requires a certain minimum spacing between two selected grid cells depending on the source dimensions.

In this study, in order to obtain a sparse solution, reweighted l_1-norm minimization technique [21] is applied with a defined cardinality ($N_s = \sum w_i$) of $\mathbf{w} \in R^{N_g}$ that represents the desired number of sources in the final layout. A constraint on the inter-element spacing is also defined as proposed by D'Urso et al. [23] to prevent overlapping. Thus, considering the objective function defined in Eq. (9), the algorithm objective at iteration-j becomes

$$\begin{aligned} &\text{minimize} |Z^{(j)} * (T_{\text{ref}}.\mathbf{w})|_1 \quad s.t. \\ &\mathbf{0} \leqslant \mathbf{w} \leqslant \mathbf{1} \\ &\sum_{i=1}^{N_g} w_i = N_s \\ &S * \mathbf{w} \leqslant \mathbf{1} \\ &Z_i^{(j)} = \frac{1}{w_i^{(j-1)} + \epsilon}, \quad i = 1, 2, \ldots, N_g \end{aligned} \tag{10}$$

where "." represents the dot product of two vectors and "*" represents the matrix product. Z is a diagonal weighting matrix whose nonzero elements are given by the reciprocal of the sum of the corresponding weights from the previous iteration and ϵ. To have good convergence and stability, ϵ should be set slightly smaller than the expected non-zero values of the entries of $\mathbf{w}$ [21]. It also ensures that a zero value in $\mathbf{w}^j$ does not prevent a nonzero estimate in the next iteration. S is an N_g x N_g matrix defined as the "separation" matrix. For square-shaped heat sources, S centers a square of side lengths equal to the guaranteed minimum inter-source spacing (d_g) whose inside is filled with ones and outside with zeros. The minimum spacing of the sources in the final layout (d_{min}) may be larger than the guaranteed spacing that is given as an input parameter.

The optimization problem in Eq. (10) is a nonlinear convex problem, namely a second-order cone programming (SOCP) problem [26]. Thus, it can be efficiently solved by many commercially available solvers (such as CVX [27]) using interior point methods. The solution time of such a process is approximately the same with a linear problem of equivalent size.

4. Results and discussion

4.1. Parameters of the cases

In this section, the parameters for the layout optimization problem are provided. Since the convex optimization algorithm is proposed as an alternative to the existing methods, the scenarios and design parameters applied by Chen et al. [18–20] are taken as a reference in the first three cases. In the last case, a Volume-to-Volume (VV) problem is introduced, which has not been investigated before in the existing layout optimization techniques.

Table 1
Optimized results in Case 1 for a coarse ($N_g = 37^2$) and a fine ($N_g = 91^2$) grid for the heat source placement.

Spacing of the square grid (m)	0.0025	0.001
Number of grid cells, N_g	37×37	91×91
Guaranteed min. spacing, d_g (m)	0.01	0.01
Number of iterations	1	3
Normalized max. temperature rise, R_m	0.2983	0.3081
Max. temperature, $T_{\max}$ (K)	327.83	328.81
Normalized std., σ_m ($\times 10^{-2}$)	1.4263	1.5585
Min. distance between the sources, $d_{\min}$ (m)	0.01	0.012
Optimization time, t_{opt} (s)	1.82	537.31

Throughout the study of the first three cases, optimization of 20 heat sources ($N_s = 20$) in a square domain with the side length (L) of 0.1 m is aimed. The side length of a single square-shaped heat source (l) is chosen as 0.01 m with an intensity (ϕ_0) of 10,000 W/m^2. The thermal conductivity (k) equals 1 W/(m·K) for both the domain and the heat source. The first three cases studied in this paper are explained as follows.

- Case 1: Volume-to-Point (VP) problem. The cooling is via a 0.001 m wide heat sink located in the middle of the south boundary with uniform temperature at 298 K (Dirichlet BC). The other boundaries are adiabatic (Neumann BC).
- Case 2: Volume-to-Boundary (VB) problem. The cooling is from all the boundaries that are isothermal with uniform temperature at 298 K (Dirichlet BC).
- Case 3: Volume-to-Boundary (VB) problem. The cooling is from the south and west boundaries. The south boundary is isothermal and uniform at 298 K (Dirichlet BC) while the west is convective with heat transfer coefficient 5 W/(m^2·K) and the fluid temperature is 298 K (Robin BC). The other boundaries are adiabatic (Neumann BC).

The fourth case is described as follows.

- Case 4: Volume-to-Volume (VV) problem. Similar to Case 1, the cooling is via a 0.001 m wide heat sink located in the middle of the south boundary with uniform temperature at 298 K. East, west and north boundaries are adiabatic. The difference now is that the domain surface has an emissivity coefficient equal to 0.1.

In the fourth case, a 3D model is constructed and simulated in CST Mphysics Studio (CST MPS) using the thermal stationary solver. The idea is to obtain the reference temperature distribution (T_{ref}) from CST and use it at the input of the convex optimization algorithm. With the resulting source locations, the optimized temperature field is computed again in CST. The values of N_s, L, l and k are selected the same as the ones in the first three cases. To create the 3D model, a thickness of $\Delta = 0.001$ m is applied for the domain and the heat sources. Since it is not possible to define mixed boundary conditions in CST, the heat sink is realized by extending the length of the middle piece of the south boundary (which has 0.001 m width for the heat sink) by $\delta = 10^{-6}$ m. All the other boundaries are set as adiabatic. The volume density of each source (Φ_0) is set to 14,400 W/m^3 in order to match the temperature distribution result obtained in MATLAB in the case of no surface heat emission (Case 1). The background is vacuum and the ambient temperature is equal to 298 K. The emissivity coefficient is defined at the upper surface of the domain.

In all the cases, the parameter ϵ in Eq. (10) is set slightly smaller than 1 although the algorithm is seen to be robust in terms of the final layout results for different choices of ϵ. N_g and d_g are varied for a coarse and a fine grid structure for the heat source placement. After several iterations of Eq. (10), a stable solution is reached where the first 20 elements with the strongest selection weights form the final layout.

Table 2
Optimized results in Case 1 for $N_g = 91^2$ with varying guaranteed min. spacing.

Guaranteed min. spacing, d_g (m)	0.012	0.011	0.009	0.008	0.007
Number of iterations	2	2	2	1	2
Normalized max. temperature rise, R_m	0.3114	0.3050	0.3005	–	–
Max. temperature, $T_{\max}$ (K)	329.14	328.50	328.05	–	–
Normalized std., σ_m ($\times 10^{-2}$)	1.7034	1.5753	1.3891	–	–
Min. distance between the sources, $d_{\min}$ (m)	0.014	0.013	0.011	–	–
Optimization time, t_{opt} (s)	302.71	329.50	211.41	–	–

Table 3
Optimized results in Case 2 for $N_g = 37^2$ with varying guaranteed min. spacing.

Guaranteed min. spacing, d_g (m)	0.01	0.0125	0.015	0.0175
Number of iterations	1	1	1	2
Normalized max. temperature rise, R_m	0.0037	0.0031	0.0030	0.0067
Max. temperature, $T_{\max}$ (K)	298.37	298.31	298.30	298.67
Normalized std., σ_m ($\times 10^{-2}$)	0.0790	0.0702	0.0709	0.1582
Min. distance between the sources, $d_{\min}$ (m)	0.01	0.015	0.0175	0.02
Optimization time, t_{opt} (s)	1.58	1.88	2.29	5.32

Table 4
Optimized results in Case 2 for $N_g = 91^2$ with varying guaranteed min. spacing.

Guaranteed min. spacing, d_g (m)	0.015	0.014	0.013
Number of iterations	1	1	1
Normalized max. temperature rise, R_m	0.0030	0.0030	0.0030
Max. temperature, $T_{\max}$ (K)	298.30	298.30	298.31
Normalized std., σ_m ($\times 10^{-2}$)	0.0720	0.0694	0.0695
Min. distance between the sources, $d_{\min}$ (m)	0.018	0.016	0.016
Optimization time, t_{opt} (s)	204.39	158.31	150.26

Table 5
Optimized results in Case 3 for $N_g = 91^2$ with varying guaranteed min. spacing.

Guaranteed min. spacing, d_g (m)	0.011	0.01	0.009	0.008
Number of iterations	2	4	1	2
Normalized max. temperature rise, R_m	0.0328	0.0306	0.0272	–
Max. temperature, T_{max} (K)	301.28	301.06	300.72	–
Normalized std., σ_m ($\times 10^{-2}$)	0.6478	0.6976	0.4300	–
Min. distance between the sources, d_{min} (m)	0.012	0.012	0.011	–
Optimization time, t_{opt} (s)	279.70	685.39	99.93	–

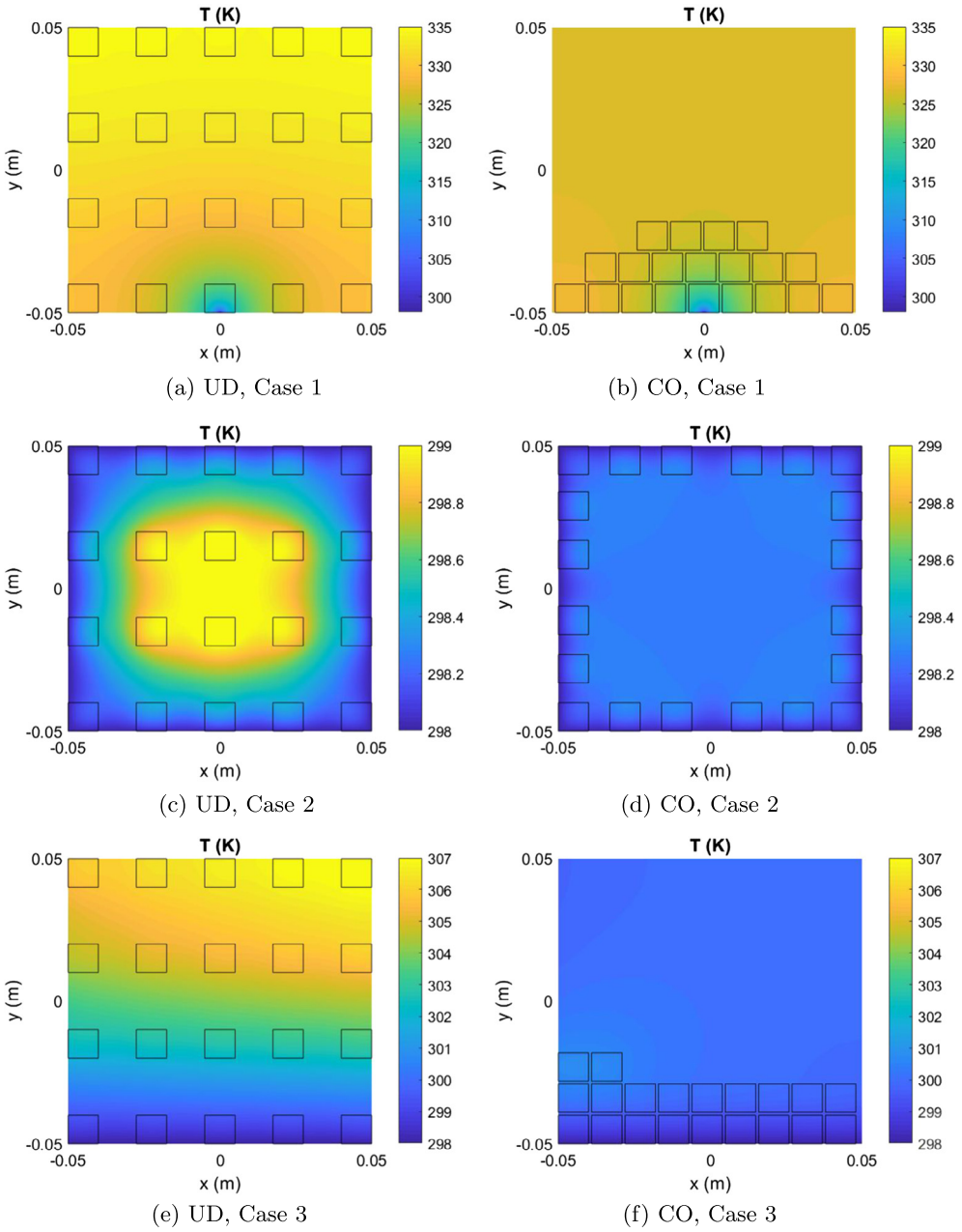

(a) UD, Case 1 (b) CO, Case 1

(c) UD, Case 2 (d) CO, Case 2

(e) UD, Case 3 (f) CO, Case 3

Fig. 1. Uniform (UD) and convex-optimized (CO) distribution of 20 heat sources in the first three cases.

All simulations are carried out on an Intel(R) Core(TM) i7-4710HQ 2.5 GHz CPU, 16 GB RAM computer using CVX and MATLAB. In Case 4, CST MPS is also used for 3D simulations.

To have sufficient resolution within a reasonable time, the number of samples for the temperature field calculations is taken as 1000×1000 ($N_T = 10^6$). Note that for the convex optimization algorithm, the temperature field is calculated only once using a uniform heat generation in order to obtain the reference temperature distribution (T_{ref}) at the algorithm input. For the selected N_T, the reference temperature field calculation time (t_{ref}) is about 9–10 s for all the three cases. After the optimization of 20 heat sources, the resulting temperature field is computed in t_T, which

Table 6
Comparison of performance for the uniform and optimized heat source layouts in the first three cases.

	UD			CO		
	R_m	T_{max}	σ_m ($\times 10^{-2}$)	R_m	T_{max}	σ_m ($\times 10^{-2}$)
Case 1:	0.3694	334.94	3.3365	0.3005	328.05	1.3891
Case 2:	0.0115	299.15	0.3185	0.0030	298.30	0.0694
Case 3:	0.0939	307.39	2.5421	0.0272	300.72	0.4300

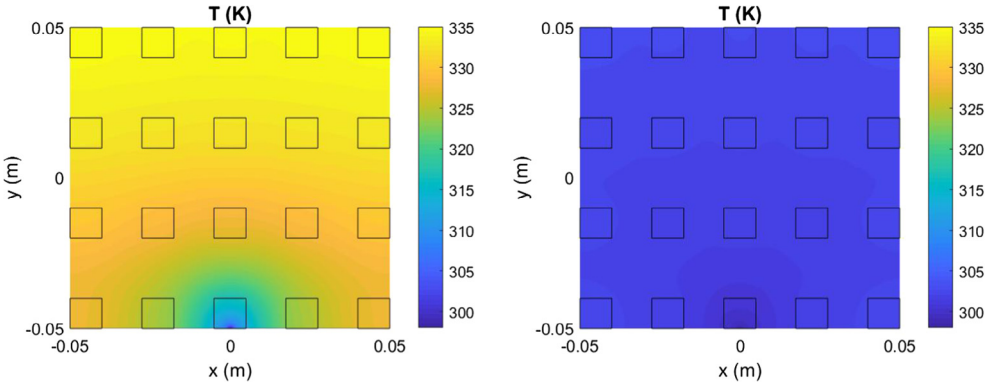

(a) UD, Case 1 (no emission) (b) UD, Case 4 (with $\varepsilon = 0.1$)

Fig. 2. Temperature field results from CST MPS for uniform distribution (UD) of 20 heat sources in Case 1 and Case 4.

Table 7
Optimized results in Case 4 for $N_g = 91^2$ with varying guaranteed min. spacing.

Guaranteed min. spacing, d_g (m)	0.018	0.016	0.014	0.012
Number of iterations	3	5	2	2
Max. temperature, T_{max} (K)	302.58	302.83	302.89	302.89
Std., σ	0.2768	0.3202	0.8318	0.9886
Min. distance between the sources, d_{min} (m)	0.021	0.019	0.016	0.014
Optimization time, t_{opt} (s)	1822.40	2133.38	543.91	410.91

is about 160–180 s for Case 1 and Case 3 and 60–80 s for Case 2. In Case 4, each temperature field computation in CST MPS takes about 25 s.

4.2. Discussion of the results

Table 1 shows the input parameters (N_g and d_g) and convex optimization results ($R_m, T_{max}, \sigma_m, d_{min}$ and t_{opt}) in Case 1 for a coarse and a fine grid for the heat source placement. The guaranteed minimum inter-spacing, d_g is equal to the side length of a single heat source.

It is seen that T_{max} and σ_m are both lower in the coarse grid ($N_g = 37^2 = 1369$) compared to the fine grid ($N_g = 91^2 = 8281$). This implies that the result for the coarse grid is more favorable. However, it is also observed that the resulting minimum inter-source spacing, d_{min} is larger than 0.01 m (i.e. the smallest value allowable) for the fine grid. This shows the input parameter d_g can be varied in the fine grid to seek for a better result. Table 2 provides the results of this analysis. Note that "–" sign in Table 2 indicates that there is no feasible solution due to the overlapping heat sources in the final layout.

When the results in Tables 1 and 2 are compared, it can be inferred that the best layout among them is obtained when the fine grid is used with $d_g = 0.009$ m. Although T_{max} is lower for the coarse grid, this selection lowers the standard deviation significantly while yielding a comparable maximum temperature value.

Next, a similar study is performed for Case 2 applying the same coarse and fine source placement grids as in Case 1 and using several different d_g values as inputs. The results are summarized in Tables 3 and 4 for the coarse and fine grid, respectively.

According to Table 3, taking $d_g = 0.015$ m yields the best solution for the coarse grid. However, using a finer grid gives the opportunity to define a finer step for d_g (through the solution of the inter-element spacing constraint in Eq. (10)), which could provide a better solution. This is indeed the case since an improved optimization result is observed in Table 4 for the fine grid with $d_g = 0.014$ m.

Having seen the usefulness of applying a fine grid for the heat source placement in Case 1 and Case 2, only the fine grid results with varying d_g values are given for Case 3 in Table 5. As previously stated, the "–" sign means overlapping in the final layout, which is not allowed.

According to Table 5, the best solution among the tested scenarios in Case 3 is obtained when d_g is equal to 0.009 m.

The optimized heat source layouts for the first three cases with 20 sources and their respective temperature field distributions are provided in Fig. 1 together with the results of uniformly distributed heat sources. The uniform distribution is described as in [18] where the domain is covered by 5 equi-spaced source repetitions in the horizontal and 4 equi-spaced source repetitions in the vertical direction.

The comparison of the convex optimization and uniform distribution results is given in Table 6 for completeness. It is seen that

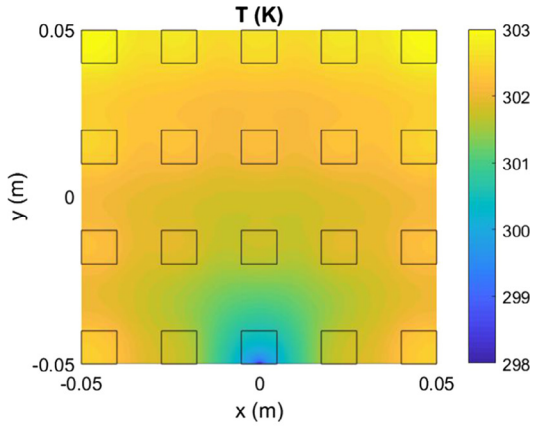

(a) UD, Case 4

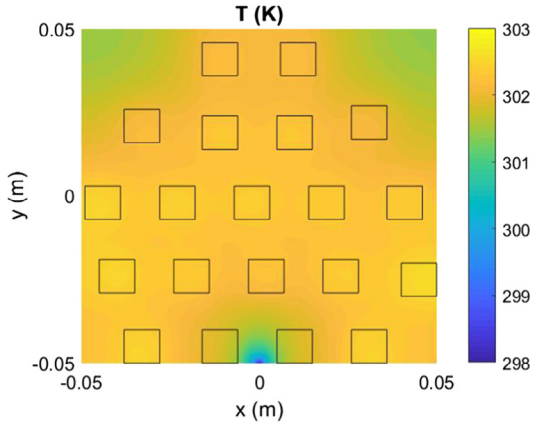

(b) CO, Case 4

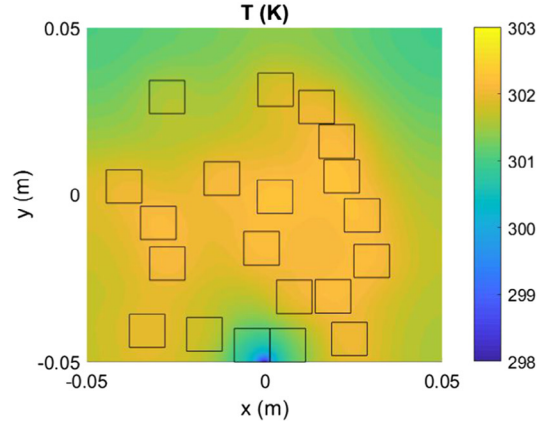

(c) GA, Case 4

Fig. 3. The layouts of 20 heat sources and temperature distributions for uniform distribution (UD), convex optimization (CO) and genetic algorithm (GA) in Case 4.

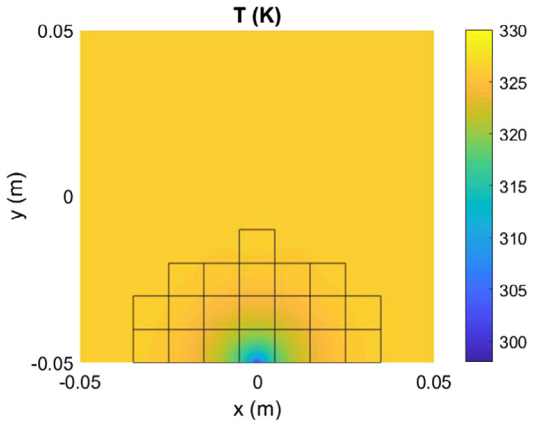

(a) BO, Case 1 (Chen et al. [18])

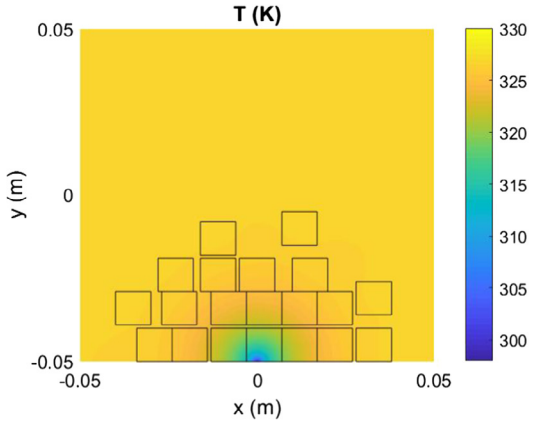

(b) SA, Case 1 (Chen et al. [20])

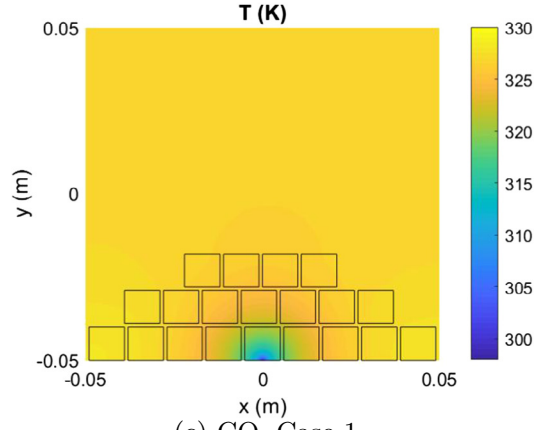

(c) CO, Case 1

Fig. 4. Optimized layouts of 20 heat sources for bionic optimization (BO), simulated annealing (SA) and convex optimization (CO) in Case 1.

Table 8
Comparison of the optimized layouts and the uniform layout in Case 4 for different methods ($N_s = 20$).

UD		CO		GA	
T_{max} (K)	σ	T_{max} (K)	σ	T_{max} (K)	σ
303.02	0.4754	302.58	0.2768	302.25	0.3496

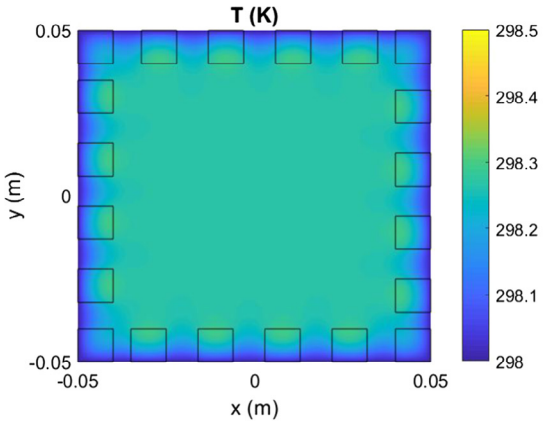

(a) BO, Case 2 (Chen et al. [18])

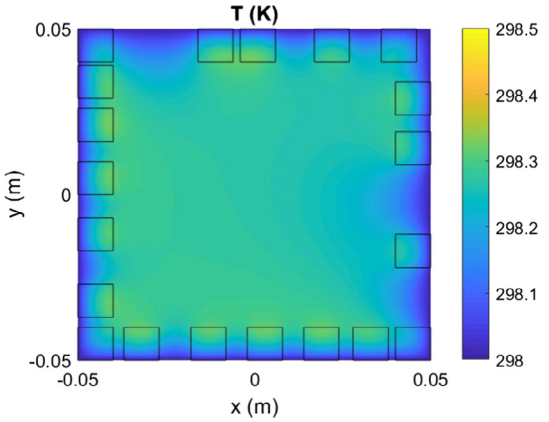

(b) SA, Case 2 (Chen et al. [20])

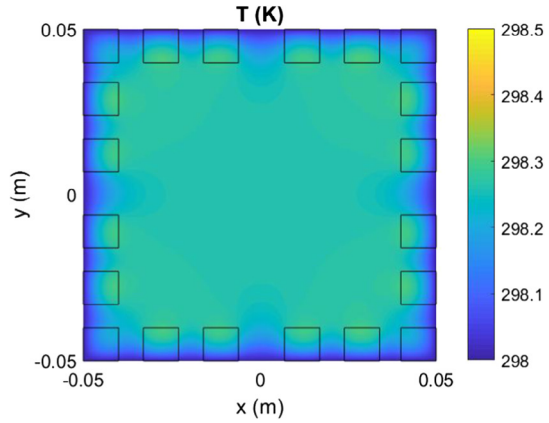

(c) CO, Case 2

Fig. 5. Optimized layouts of 20 heat sources for bionic optimization (BO), simulated annealing (SA) and convex optimization (CO) in Case 2.

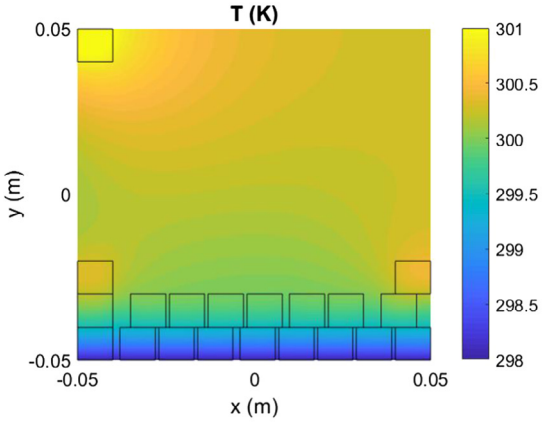

(a) BO, Case 3 (Chen et al. [18])

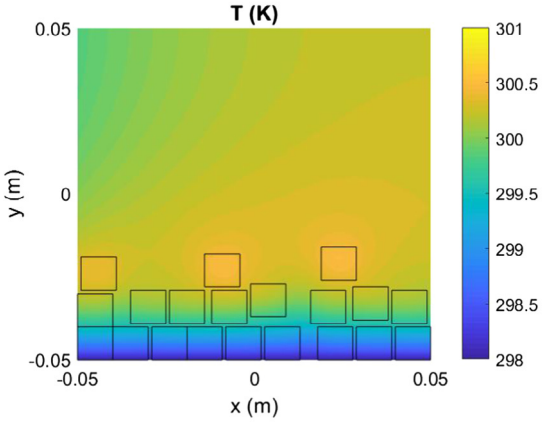

(b) SA, Case 3 (Chen et al. [20])

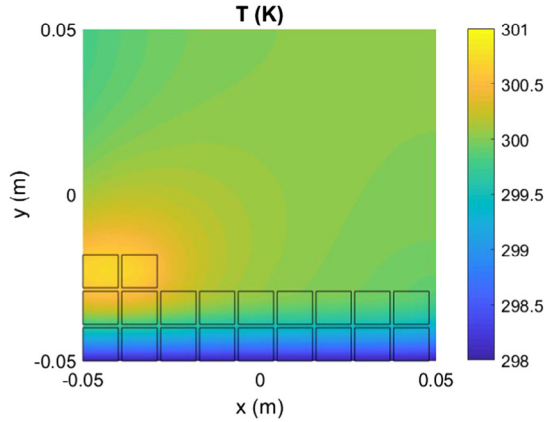

(c) CO, Case 3

Fig. 6. Optimized layouts of 20 heat sources for bionic optimization (BO), simulated annealing (SA) and convex optimization (CO) in Case 3.

via convex optimization, the normalized maximum temperature rises (R_m) in Case 1, Case 2 and Case 3 are reduced by 18.65%, 73.91% and 71.03%, respectively, when compared to the uniform distribution. Besides, the values of the normalized standard deviations (σ_m) are reduced by 58.37%, 78.21% and 83.08% in Case 1, Case 2 and Case 3, respectively.

Fig. 2 shows the results of CST MPS simulations for the 'imitated' version of Case 1 with a heat sink in the middle of the south boundary for the uniform source layout and the effect of considering the surface emission in such a scenario, which represents Case 4. If the heat emission is absent (Fig. 2a), the CST simulation results in the same temperature distribution as shown in Fig. 1a, and thus verifies the CST simulation model. After defining the surface emissivity $\varepsilon = 0.1$, the maximum temperature of the domain is reduced to 303.02 K (see Fig. 2b). Using the temperature distribution in Fig. 2b as T_{ref}, the source positions are optimized using the proposed convex optimization (CO) algorithm. The results are pro-

Table 9
Comparison of the optimization results in the first three cases for different methods ($N_s = 20$).

	BO		SA		CO	
	R_m	σ_m ($\times 10^{-2}$)	R_m	σ_m ($\times 10^{-2}$)	R_m	σ_m ($\times 10^{-2}$)
Case 1:	0.2820	1.2753	0.2866	1.3730	0.3005	1.3891
Case 2:	0.0030	0.0694	0.0033	0.0745	0.0030	0.0694
Case 3:	0.0312	0.4976	0.0249	0.4605	0.0272	0.4300

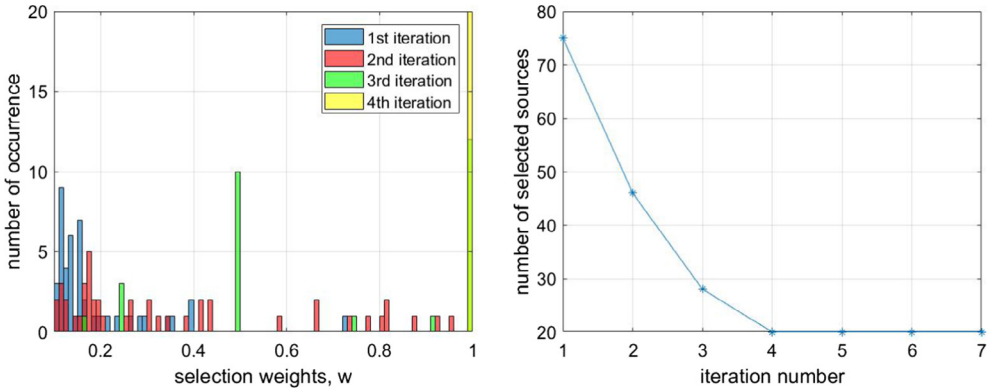

(a) Histogram of source selection weights at each iteration

(b) Number of selected sources at each iteration

Fig. 7. Convergence analysis of the convex optimization algorithm in Case 3 with d_g = 0.01 m.

vided in Table 7 which show that the lowest maximum temperature and standard deviation in Case 4 is obtained when d_g is equal to 0.018 m.

In order to have a comparative study, the built-in genetic algorithm (GA) of CST is also used for the layout optimization in Case 4 with the aim of minimizing the maximum temperature. In GA, 120 iterations are used to obtain the final result where each iteration takes about 25 s. Fig. 3 gives the source locations and temperature distributions for the uniform distribution (UD), convex optimization (CO) and genetic algorithm (GA). The comparison results of these three approaches are summarized in Table 8. It is seen that CO and GA can provide a slight reduction in the maximum temperature, but the change is not noticeable for the selected parameters. On the other hand, optimized solutions possess much more uniform temperature distributions (with temperature standard deviation reduction by 41.78% and 26.46% for CO and GA, respectively).

Next, the results of the first three cases are compared with the results of the existing layout optimization methods, namely bionic optimization (BO) [18] and simulated annealing (SA) [20]. In Figs. 4–6, the source location and temperature field distribution comparisons between these methods and the convex optimization (CO) are provided for Case 1, Case 2 and Case 3, respectively. The comparison results of these three methods are summarized in Table 9.

In Case 1, the performance of CO is worse than BO and SA. In CO, R_m is increased by 6.56% and 4.85% and σ_m is increased by 8.92% and 1.17% when compared to BO and SA, respectively. In Case 2, CO achieves the same results with BO and it performs better than SA. Compared to SA, R_m and σ_m are reduced by 9.09% and 6.85%, respectively. In Case 3, CO outperforms BO by decreasing R_m and σ_m by 12.82% and 13.59%, respectively. When compared to SA, although R_m increases by 9.24%, σ_m is reduced by 6.62% leading to a more uniform temperature distribution.

The computational costs for BO and SA are given in [20] in terms of the total number of temperature field calculations. It is stated that for 20 heat sources, the total number of temperature field calculations, which is proportional to the number of sources, is 420 and 1760 for BO and SA, respectively. On the other hand, in CO, the temperature field is calculated only once in order to obtain the reference temperature field with uniform heat generation in the domain. Besides, the optimization time does not depend on the number of sources. In fact, in CO, the main factors affecting the optimization time are the number of grid cells for placing the heat sources (N_g) and the required number of iterations.

Lastly, the convergence of the convex optimization algorithm is shown in Fig. 7 for the case that requires the most number of iterations among all the cases studied in the paper (Case 3 for $N_g = 91^2$ and d_g = 0.01 m with 4 iterations, as seen in Table 5). In Fig. 7a, the histogram plot of the heat source selection weights (that are larger than 0.1) is given up to the fourth iteration. Assuming that a source with a selection weight larger than 0.1 is 'active' (or 'selected'), the number of selected sources at each iteration is plotted in Fig. 7b. It is seen that as iteration number increases, less sources are selected. Besides, larger weights are assigned to satisfy the cardinality constraint, which provides the increased sparsity. At the fourth iteration, the number of active sources converges to 20 when 20 sources are selected with weight 1 and the result does not change afterwards.

5. Conclusions

In this paper, cooling enhancement via heat source distribution optimization for two dimensional heat conduction problem was studied. Using the convex algorithm, a new approach to decrease the maximum temperature and temperature non-uniformity was proposed. This solution is based on obtaining a sparse solution from a fully-populated heat source array while keeping the predefined number of sources at potentially easy-to-cool regions of the domain.

On top of being easy to implement, the proposed convex optimization algorithm was seen to provide comparable or better results than the existing methods in terms of the maximum temperature and temperature uniformity. Moreover, convex optimization requires only a single temperature field calculation to be used as a reference, while for the existing methods, the number of temperature field calculations are proportional to the number of sources.

Three test cases with different boundary conditions were revised to evaluate the performance of the proposed layout optimization algorithm, and the results were compared with the uniform distribution of 20 heat sources. In all cases, it was seen that using iterative reweighted l_1-norm convex minimization, the maximum temperature of the domain can be effectively reduced.

The fourth case, representing a more realistic 3D situation, took the heat emission from the domain surface into account. Convex optimization (CO) and genetic algorithm (GA) were used to optimize the positions of the heat sources and the results were compared with the uniformly distributed (UD) layout. The results indicated that for the selected surface emissivity coefficient, heat emission from the surface becomes the dominant cooling mechanism which is further enhanced by the conduction cooling. That is why the highest temperature value is almost the same (slightly improved) for CO and GA when compared to UD, but much better temperature uniformity can be achieved via layout optimization.

The sequential reweighted l_1-norm convex minimization technique can be applied in a straightforward way to deal with larger number of heat sources or with different boundary conditions. In general, it is an efficient and effective method to optimize the heat source layout and enhance the cooling performance in two dimensional heat conduction problems.

Conflict of interest

We wish to confirm that there are no known conflicts of interest associated with this publication.

Acknowledgment

This research was conducted as part of the STW-NXP Partnership Program on Advanced 5G Solutions within the project titled “Antenna Topologies and Front-end Configurations for Multiple Beam Generation”. For further information: www.nwo.nl.

Appendix A. Supplementary material

Supplementary data associated with this article can be found, in the online version, at https://doi.org/10.1016/j.ijheatmasstransfer.2018.02.001.

References

[1] P. Mankowski, A. Dominiak, R. Domanski, M.J. Kruszewski, L. Ciupinski, Thermal conductivity enhancement of copper-diamond composites by sintering with chromium additive, J. Therm. Anal. Calorim. 116 (2) (2014) 881–885, https://doi.org/10.1007/s10973-013-3604-3.

[2] J. Fukai, M. Kanou, Y. Kodama, O. Miyatake, Thermal conductivity enhancement of energy storage media using carbon fibers, Energy Convers. Manage. 41 (14) (2000) 1543–1556, https://doi.org/10.1016/S0196-8904(99)00166-1.

[3] A. Bejan, Constructal-theory network of conducting paths for cooling a heat generating volume, Int. J. Heat Mass Transfer 40 (4) (1997) 799–811, https://doi.org/10.1016/0017-9310(96)00175-5.

[4] L. Ghodoossi, Conceptual study on constructal theory, Energy Convers. Manage. 45 (9) (2004) 1379–1395, https://doi.org/10.1016/j.enconman.2003.09.002.

[5] L. Chen, Progress in study on constructal theory and its applications, Sci. China Technol. Sci. 55 (3) (2012) 802–820, https://doi.org/10.1007/s11431-011-4701-9.

[6] Z. Guo, H. Zhu, X. Liang, Entransy a physical quantity describing heat transfer ability, Int. J. Heat Mass Transfer 50 (13) (2007) 2545–2556, https://doi.org/10.1016/j.ijheatmasstransfer.2006.11.034.

[7] Q. Chen, H. Zhu, N. Pan, Z. Guo, An alternative criterion in heat transfer optimization, Proc. Roy. Soc. A: Math. Phys. Eng. Sci. 467 (2128) (2011) 1012–1028, https://doi.org/10.1098/rspa.2010.0293.

[8] Q. Chen, X. Liang, Z. Guo, Entransy theory for the optimization of heat transfer – a review and update, Int. J. Heat Mass Transfer 63 (2013) 65–81, https://doi.org/10.1016/j.ijheatmasstransfer.2013.03.019.

[9] X. Cheng, Z. Li, Z. Guo, Constructs of highly effective heat transport paths by bionic optimization, Sci. China Ser. E: Technol. Sci. 46 (3) (2003) 296–302, https://doi.org/10.1360/03ye9032.

[10] Z. Xia, X. Cheng, Z. Li, Bionic optimization of heat transport paths for heat conduction problems, J. Enhanc. Heat Transfer 11 (2) (2004) 119–132, https://doi.org/10.1615/JEnhHeatTransf.v11.i2.20.

[11] X. Xu, X. Liang, J. Ren, Optimization of heat conduction using combinatorial optimization algorithms, Int. J. Heat Mass Transfer 50 (9) (2007) 1675–1682, https://doi.org/10.1016/j.ijheatmasstransfer.2006.10.037.

[12] X. Cheng, X. Xu, X. Liang, Homogenization of temperature field and temperature gradient field, Sci. China Ser. E: Technol. Sci. 52 (10) (2009) 2937–2942, https://doi.org/10.1007/s11431-009-0244-8.

[13] R.R. Madadi, C. Balaji, Optimization of the location of multiple discrete heat sources in a ventilated cavity using artificial neural networks and micro genetic algorithm, Int. J. Heat Mass Transfer 51 (9) (2008) 2299–2312, https://doi.org/10.1016/j.ijheatmasstransfer.2007.08.033.

[14] T.V.V. Sudhakar, C. Balaji, S.P. Venkateshan, Optimal configuration of discrete heat sources in a vertical duct under conjugate mixed convection using artificial neural networks, Int. J. Therm. Sci. 48 (5) (2009) 881–890, https://doi.org/10.1016/j.ijthermalsci.2008.06.013.

[15] T.K. Hotta, C. Balaji, S.P. Venkateshan, Optimal distribution of discrete heat sources under mixed convection a heuristic approach, J. Heat Transfer 136 (10) (2014) 104503, https://doi.org/10.1115/1.4027350.

[16] T.K. Hotta, C. Balaji, S.P. Venkateshan, Experiment driven ann-ga based technique for optimal distribution of discrete heat sources under mixed convection, Exp. Heat Transfer 28 (3) (2015) 298–315, https://doi.org/10.1080/08916152.2013.871867.

[17] S. Soleimani, D.D. Ganji, M. Gorji, H. Bararnia, E. Ghasemi, Optimal location of a pair heat source-sink in an enclosed square cavity with natural convection through pso algorithm, Int. Commun. Heat Mass Transfer 38 (5) (2011) 652–658, https://doi.org/10.1016/j.icheatmasstransfer.2011.03.004.

[18] K. Chen, S. Wang, M. Song, Optimization of heat source distribution for two-dimensional heat conduction using bionic method, Int. J. Heat Mass Transfer 93 (2016) 108–117, https://doi.org/10.1016/j.ijheatmasstransfer.2015.09.041.

[19] K. Chen, S. Wang, M. Song, Temperature-gradient-aware bionic optimization method for heat source distribution in heat conduction, Int. J. Heat Mass Transfer 100 (2016) 737–746, https://doi.org/10.1016/j.ijheatmasstransfer.2016.05.011.

[20] K. Chen, J. Xing, S. Wang, M. Song, Heat source layout optimization in two-dimensional heat conduction using simulated annealing method, Int. J. Heat Mass Transfer 108 (2017) 210–219, https://doi.org/10.1016/j.ijheatmasstransfer.2016.12.007.

[21] E.J. Candes, M.B. Wakin, S.P. Boyd, Enhancing sparsity by reweighted l1 minimization, J. Fourier Anal. Appl. 14 (5) (2008) 877–905, https://doi.org/10.1007/s00041-008-9045-x.

[22] M. D'Urso, G. Prisco, Maximally sparse arrays via sequential convex optimizations, IEEE Anten. Wirel. Propag. Lett. 11 (2012) 192–195, https://doi.org/10.1109/LAWP.2012.2186626.

[23] M. D'Urso, G. Prisco, R.M. Tumolo, Maximally sparse, steerable, and nonsuperdirective array antennas via convex optimizations, IEEE Trans. Anten. Propag. 64 (9) (2016) 3840–3849, https://doi.org/10.1109/TAP.2016.2586490.

[24] S.E. Nai, W. Ser, Z.L. Yu, H. Chen, Beampattern synthesis for linear and planar arrays with antenna selection by convex optimization, IEEE Trans. Anten. Propag. 58 (12) (2010) 3923–3930, https://doi.org/10.1109/TAP.2010.2078446.

[25] A.S. Reimer, A.F. Cheviakov, A matlab-based finite-difference solver for the poisson problem with mixed Dirichlet-Neumann boundary conditions, Comput. Phys. Commun. 184 (3) (2013) 783–798, https://doi.org/10.1016/j.cpc.2012.09.031.

[26] M. Lobo, L. Vandenberghe, S. Boyd, H. Lebret, Applications of second-order cone programming, Linear Algeb. Appl. 284 (1–3) (1998) 193–228, https://doi.org/10.1016/S0024-3795(98)10032-0.

[27] M. Grant, S. Boyd, CVX: Matlab Software for Disciplined Convex Programming, Version 2.1, 2014. <http://cvxr.com/cvx>.